Theor Chem Acc (2007) 117:699–707
DOI 10.1007/s00214-006-0202-5

REGULAR ARTICLE

Theoretical mechanistic studies on oxidation reactions of some saturated and unsaturated organic molecules

G. Ghigo · A. Maranzana · M. Causà · G. Tonachini

Received: 4 September 2006 / Accepted: 13 October 2006 / Published online: 13 December 2006

Abstract This account describes the results collected by our group during the last years on some themes of environmental/mechanistic interest. Theoretical quantum-mechanical investigations have been carried out to help clarifying the mechanism of some oxidation reactions, which involve mainly unsaturated but also saturated organics as substrates, and, as reactive oxidants, triplet or singlet dioxygen, hydroxyl, ozone, and nitrogen oxides. Depending on the problem, the calculations are either multi-configurational (as CAS-MCSCF, CAS-PT2, MC-QDPT2), or based on the Density Functional Theory for the heavier systems. Research work has thus been developed along the following lines: hydrocarbon oxidations under atmospheric or combustion conditions; definition of a model for soot particles and their interaction with species as HO, O_2, O_3, NO, NO_2, NO_3, etc.; investigation on the reaction mechanism of $^1\Delta_g$ dioxygen with organic unsaturated systems (cycloaddition and *ene* reactions).

Keywords Hydrocarbons · Atmospheric oxidation · Combustion · Soot · Singlet dioxygen

G. Ghigo · A. Maranzana · G. Tonachini (✉)
Dipartimento di Chimica Generale ed Organica Applicata,
Università di Torino, Corso Massimo D'Azeglio 48,
10125 Torino, Italy
e-mail: glauco.tonachini@unito.it
URL: http://www.thecream.unito.it

M. Causà
Dipartimento di Scienze dell'Ambiente e della Vita
DISAV, Università del Piemonte Orientale
"Amedeo Avogadro", Piazza Ambrosoli 5,
15100 Alessandria, Italy

During the last years our group has been working on some topics of environmental and mechanistic interest. Organic reactions of unsaturated and saturated molecules have been investigated by theoretical instruments. All these processes are oxidations, and the chief oxidant is the oxygen molecule, though other molecules too, as hydroxyl, ozone, or the nitrogen oxides, play important roles. The reactions studied are either atmospheric and combustion hydrocarbon oxidations, in which ground state triplet ($^3\Sigma_g$) dioxygen intervenes, or cycloaddition and *ene* reactions in which the oxidant is the first electronically excited degenerate state $^1\Delta_g$ of dioxygen. Moreover, we have looked for a suitable definition of a model for soot particles and investigated their interaction with species as HO, $^3O_2$, NO, NO_2, NO_3, and, in particular, O_3. In all cases our main goal has been to give a contribution to elucidate the mechanistic details of the reactions considered. To this end, theoretical quantum-mechanical calculations have been carried out, which are, depending on the problem, either multi-configurational [namely the Complete Active Space (CAS) variant of the Multi-Configuration Self-Consistent Field (MCSCF) theory and two related multi-reference second-order perturbative calculations (MR-PT2), the CAS-PT2 method and the MC-QDPT2 (quasi-degenerate) method] [1–8] or based on the Density Functional Theory (DFT) [9–14].

Most of the species implicated in the tropospheric reactions are radicals. Classical single-reference ab initio methods of widespread use (as Hartree–Fock or MPn) can be subject to significant spin contamination when dealing with open-shell systems. In some cases this negative aspect can be serious. DFT methods suffer this problem not as much. However, they can demonstrate some inaccuracy when dealing with radical hydrogen transfer

processes [15–20]. A multi-reference perturbative approach can be a more dependable choice: an example could be a CAS-PT2 energy calculation carried out resting on a CAS-MCSCF wave-function and geometry optimization. Unfortunately, this approach is computationally demanding, and would be manageable only for systems of rather limited size. Having in mind a likely extension to moderately large organic systems, our first point was to assess which theory level could be affordable and yield trustworthy results at the same time. This is a rather delicate point, and a compromise solution was expected, a trade off between feasibility and reliability.

One simple reaction was then selected and studied by different quantum-mechanical methods, to compare the results provided by different levels of theory [21]. The DFT, using the popular B3LYP functional [DFT (B3LYP)], Møller–Plesset theory up to the fourth-order [MP2-MP4], and Coupled Cluster methods [CCSD(T)] were used. Moreover, the mentioned CAS-MCSCF, CAS-PT2, and MC-QDPT2 methods were also used.

The reaction chosen is the following hydrogen-abstraction: $^3\Sigma_g O_2 + HOCH_2CH_2^{\bullet} \rightarrow HOO^{\bullet} + HOCH{=}CH_2$, which converts the simplest β-hydroxy radical to an enol. It models for instance the one-step transformation of hydroxycyclohexadienyl radical into phenol by O_2. UDFT(B3LYP), UMP2 (where U stays for unrestricted), and CAS-MCSCF optimizations were first carried out to define the stable and transition structures. In a second phase, the energetics were assessed more accurately by spin-projected (P) single-reference PMP4//UMP2 calculations (which were compared with CCSD(T)//UMP2 results), and by two multi-reference second-order perturbation methods (MR-PT2), which are based on CAS-MCSCF wave-functions and structures. In the multi-configurational studies, a (11,9) active space and the 6-311G(d,p) basis set were chosen. The MR-PT2 estimates for the energy barrier and reaction energy were: 14.5 and $-12.1\,\mathrm{kcal\,mol^{-1}}$ (CAS-PT2), and 8.3 and $-13.4\,\mathrm{kcal\,mol^{-1}}$ (MC-QDPT2). These estimates are intermediate between the DFT(B3LYP)/6-311G(d,p) (3.3 and $-19.1\,\mathrm{kcal\,mol^{-1}}$) and PMP4/6-311G (d,p) values (17.2 and $-10.7\,\mathrm{kcal\,mol^{-1}}$). The results show that the DFT(B3LYP) method tends to underestimate the barrier for H-abstraction (this feature had also been observed in other studies [22–27], for which suitable experimental and high-level computational references were available). By contrast, the PMP4 barrier is likely to correspond to an upper limit, and this is probably due to the fact that the single-reference perturbation expansion does not converge very effectively. At the CAS-MCSCF level, the transition structure is described by a wave-function in which three configurations give significant contributions. Considering the purpose of defining a qualitatively correct reference in a perturbative calculation, the MR-PT2 approach is preferable. However, since this simple system was studied as a model for more demanding problems, we ultimately regarded DFT as the best choice for rather large systems, providing a compromise between accuracy and feasibility. As regards possible basis set effects, single point energy computations using larger basis sets [up to 6-311 + G(3df,p)] were carried out. We found that extending the basis set had a limited impact. However, some increase in reaction exoergicity and a consistent lowering of the energy barriers upon extension were observed at all theory levels.

Since non-negligible (though nowadays luckily declining) amounts of benzene are emitted in the troposphere by the combustion of the so-called "green" (lead-free) gasoline, it was of some interest to investigate the fate of this dangerous molecule in the troposphere. We pursued this goal in a few studies (carried out in the period 1998–2002) in which the oxidative degradation of benzene was investigated. Free energy profiles were defined for a series of transformations. Free energy differences were based on (i) energy differences computed at the DFT(B3LYP)/6-311+G(d,p) in correspondence of DFT (B3LYP)/6-31G(d) optimized geometries and (ii) the thermochemistry from the DFT(B3LYP)/6-31G(d) vibrational analysis.

During daytime, the most likely attack benzene may undergo in the troposphere is by the very reactive radical $HO^{\bullet}$, which has a diurnal mean concentration of the order of 10^6 molecules cm^{-3}. This first step generates the hydroxycyclohexadienyl radical intermediate **I** (Scheme 1). In the first paper on this topic [28], three different attacks of $^3\Sigma_g O_2$ on **I** were studied. Abstraction by O_2 of the hydrogen *gem* to OH in **I** ($\Delta G^{\ddagger} = 13.6\,\mathrm{kcal\,mol^{-1}}$) affords phenol, which can undergo further oxidation. On the other hand, O_2 addition to the π-delocalized system of **I** ($\Delta G^{\ddagger} = 15.6\,\mathrm{kcal\,mol^{-1}}$) produces a hydroxycyclohexadienyl peroxyl radical intermediate. Both attacks are relatively easy and open several possible channels toward further degradation. The former reaction is exothermic by $27\,\mathrm{kcal\,mol^{-1}}$, the latter only by 1, thus reversible. In contrast, a pathway proposed by some experimentalists, which would lead to benzene oxide/oxepin via hydrogen abstraction from the hydroxyl in **I** operated by O_2, was assessed as not competitive, since it shows a significantly higher barrier ($\Delta G^{\ddagger} = 39\,\mathrm{kcal\,mol^{-1}}$). Benzene oxide and oxepin were estimated to lie 21 and 19 $\mathrm{kcal\,mol^{-1}}$ above **I**, respectively.

After the study of the steps which can start benzene oxidation, we addressed the next oxidative degradation steps (ring opening included) [29]. In fact, during the tropospheric oxidation of benzene (and methylated

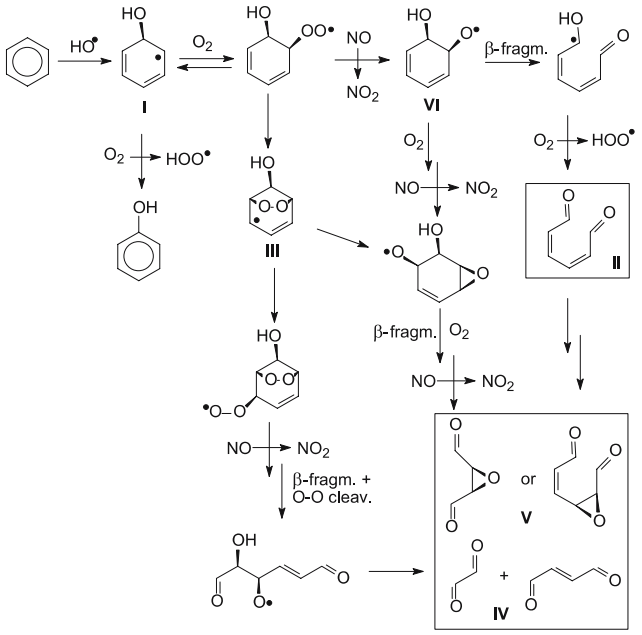

Scheme 1

benzenes), unsaturated dicarbonyls are commonly detected products. Aldehydes are known to contribute on their own to some aspects of air pollution, and hexa-2,4-dien-1,6-dial (also called muconaldehyde) (Scheme 1, box: **II**) is particularly interesting because of its toxicity. Following O_2 addition to **I**, with sufficiently high NO_x concentration (ca. 10^8–10^9 molecule cm^{-3} in non-polluted regions, up to 10^{12} in urban zones), O-abstraction by NO from the peroxyl group in the 2-hydroxycyclohexadienyl peroxyl radical can play a role. In fact, it opens a very easy cascade of oxidation steps. The first step leads to the related 2-hydroxycyclohexadienyl oxyl radical. This intermediate is prone in turn to β-fragmentation (i.e. ring opening) and generates the open-chain delocalized 6-hydroxy-hexa-2,4-dienalyl radical, which carries at one end the first carbonyl group of the final dialdehyde. The second –CHO functional group can subsequently form either by simple H abstraction operated by O_2, or by O_2 addition followed by $HOO^{\bullet}$ elimination. Both generate Z,Z-muconaldehyde **II**. The computed overall free energy drop with respect to the 2-hydroxycyclohexadienyl peroxyl radical is 48 kcal mol^{-1}. Other pathways were explored, possibly playing an important role in yielding aldehydes in case of low NO_x concentration. The results indicate that the only promising pathway is the ring closure of the 2-hydroxycyclohexadienyl peroxyl radical to the [3.2.1] bicyclic endo-peroxy allyl radical intermediate **III** ($\Delta G^{\ddagger} = 14.2$ kcal mol^{-1} with respect to the 2-hydroxycyclohexadienyl peroxyl radical). In this case, the effect of the ensuing ring opening can eventually be the production of 1,2 and 1,4 dialdehydes **IV** (i.e. the same result of a direct oxidation of muconaldehyde itself). Other intramolecular processes have been investigated and do not seem to be very promising. An attempt to estimate the relative importance of the NO-promoted and ring-closure pathways (assuming a top NO concentration as reported for polluted areas) has brought to the conclusion that the former can contribute to benzene oxidation up to less than 10% of the latter. In the case of low NO_x concentration, the monomolecular process should prevail.

We further proceeded along the same line, by investigating the formation mechanism of other unsaturated dialdehydes and their epoxides, detected when benzene undergoes oxidative degradation in the troposphere or in experiments reproducing tropospheric conditions (Scheme 1, box: **IV**, **V**) [30,31]. These toxic products are implicated in aerosol formation and in the photochemical smog chemistry. We aimed to assess the viability of some reaction channels which could either follow (a) or flank (b) the pathway to muconaldehyde just discussed. In case (a), a further oxidative degradation of muconaldehyde **II** requires the intervention of NO, and leads rather easily to glyoxal and butenedial **IV**. In case (b), the pathways examined share a common origin in an early intermediate in benzene oxidation, the 2-hydroxycyclohexadienyl peroxyl radical. A branching of the reaction pathway occurs at this point, via either a bimolecular or a monomolecular step, both irreversible. The first channel begins with the corresponding oxyl radical **VI** (in whose formation NO is involved). The second channel originates from the already seen [3.2.1] bicyclic endo-peroxy allyl-radical intermediate **III** which is generated by the closure of a peroxy bridge. This radical can generate in turn glyoxal and butenedial **IV**, while the 2-hydroxycyclohexadienyl oxyl radical can produce epoxy butenedial and epoxy muconaldehyde **V**, both through NO-mediated pathways. However, epoxy muconaldehyde can also form from the bicyclic endo-peroxy allyl-radical intermediate **III** without NO involvement. The relative importance of these channels is dependent on the concentration of NO, which is involved in the formation of **VI** but not of **III**. Of the pathways that stem from **VI** and **III**, some involve reversible initial steps and some do not. By taking into account all of these processes, four scenarios are depicted. (1) In unpolluted tropospheric conditions, the prevailing pathway is through **III**, and epoxy muconaldehyde is basically the only primary product. (2) Under polluted conditions, this situation is slightly modified, because up to 4% formation of **VI** can be predicted from our estimates. This implies that a minor amount of muconaldehyde can form along with the major product epoxy muconaldehyde. Glyoxal and butenedial can form in turn from its oxidation

as secondary products. (3) [NO] can be higher in some experiments: by setting it to 5 ppm, **VI** and **III** would form in a 4:1 ratio. Now we can surmise that muconaldehyde becomes the major product, and its formation (or that of glyoxal and butenedial as secondary products) prevails over epoxy muconaldehyde. (4) As a last scenario, an exceedingly high [NO] can be hypothesized for a local situation, as in close proximity of an exhaust source. In this case, **III** would form more slowly than **VI** (approximately by three orders of magnitude). A rising NO concentration would reinforce the formation of muconaldehyde (and then of glyoxal and butenedial), while the epoxy dialdehydes would be very minor products.

As regards the formation of oxygen-containing pentatomic cycles (especially furan, detected in the oxidation of alkylbenzenes) we found that the most likely process entails NO intervention (Scheme 2) [32].

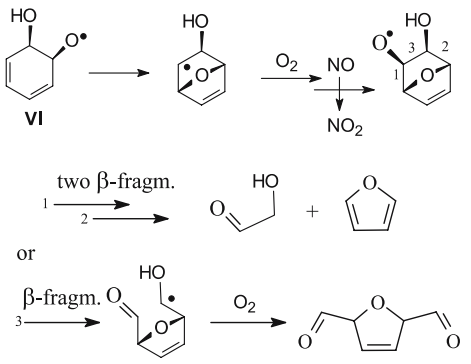

Scheme 2

Starting from **VI**, ring closure gives origin to a localized radical, which is readily attacked by O_2 (whose mean concentration is of the order of 10^{18} molecules cm^{-3}). Subsequent reduction of the peroxyl radical to oxyl by NO opens the way to two different outcomes. Either two successive β-fragmentations (cleavage of the bonds numbered 1 and 2) lead to furan, or another β-fragmentation (cleavage of the bond numbered 3) produces the dialdehyde shown in Scheme 2.

So far, we have considered the fate of unsaturated hydrocarbons (aromatics and conjugated alkenes) under conditions of tropospheric oxidative degradation; the evolution of saturated hydrocarbons is as interesting. Among alkanes, methane is in particular worthy of note, because of its relative abundance and long persistence. Alkane oxidation takes place, as was the case for the unsaturated systems, mainly by initial attack of the hydroxyl radical (hydrogen abstraction); the subsequent step is addition of the oxygen molecule, which is present, as just recalled, in a relatively abundant concentration:

$$CH_4 \xrightarrow{HO^\bullet} \dot{C}H_3 \xrightarrow{O_2} CH_3OO^\bullet.$$

The resulting alkyl peroxyls can thus form in the atmospheric oxidation of hydrocarbons, but also under combustion conditions. They can undergo different transformations, but, when NO concentration is low, they can appreciably react with themselves. This is called the self-reaction of alkyl peroxyl radicals. The reaction has both propagation and termination channels. We have carried out a mechanistic study on the simplest system, the methylperoxyl radical [33]. Multireference second-order perturbative energy calculations CAS(16,12)-PT2/6-311G(2df,p) have been carried out on the CAS(8,8)-MCSCF/6-311G(d,p) geometries pertaining to the reaction pathways explored. The self-reaction can lead to aldehydes, alcohols, and molecular oxygen. How this takes place is still a matter of discussion.

Russell, in 1957, put forward the intervention of a rather elusive intermediate, the dialkyl tetroxide, from which the products could form. Later on, the di-t-buthyltetroxide, which cannot evolve to the mentioned products because of its structure, was detected at very low temperature, trapped in an inert solid matrix. Scheme 3 summarizes our main findings about the detailed pathways of the methylperoxyl self-reaction. In our computations, $CH_3O_4CH_3$ is found as a stable energy minimum, but the calculations indicate that, as the system moves from atmospheric to combustion temperatures, its formation becomes more and more difficult.

The concerted dissociation of the two peripheral O–O bonds in the tetroxide (left) leads to the $^3(^2CH_3O^\bullet)_2 \cdots {}^3O_2$ complex, with overall singlet spin multiplicity. Within this structure, dioxygen is very loosely bound. From the complex, a H-transfer disproportionation TS would give H_2CO, CH_3OH, and O_2, and this would be a very easy termination step. It can occur in principle with production of either excited $^1O_2$ or excited ^3H_2CO, but the latter step is not favored. It can however be noticed that a large amount of energy would be released in the disproportionation, and, if $^3O_2$ is still interacting with the two methoxyl radicals, enough energy could be transferred to it to allow the formation of some $^3O_2$ (or of triplet carbonyl, in any case).

As an alternative, dissociation of the complex to $2CH_3O^\bullet + O_2$, with possible propagation, is feasible. However, a sufficiently easy intersystem crossing (ISC) could take place in the complex. This pathway could split again, and involve either dissociation to $2CH_3O^\bullet + {}^3O_2$, or H-transfer with no need for the formation of

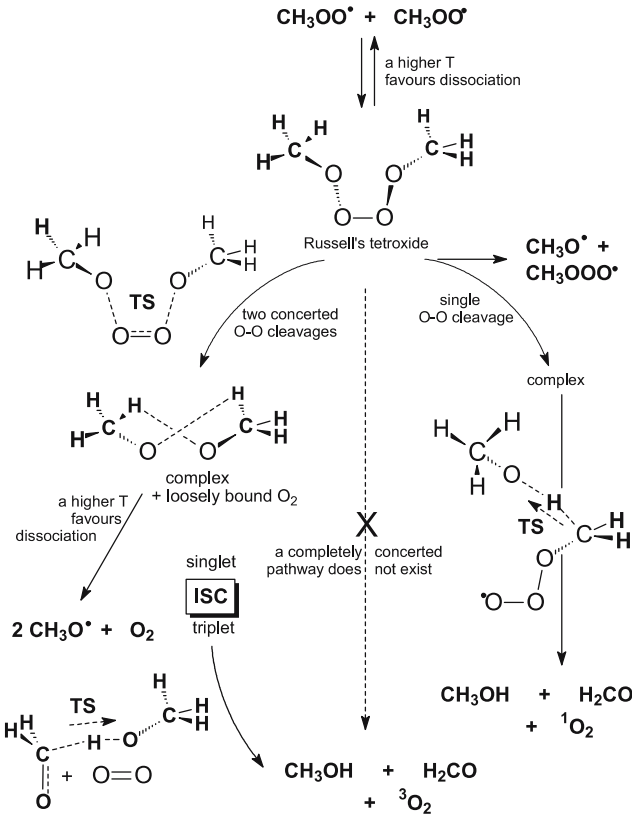

Scheme 3

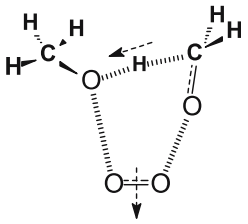

Scheme 4

singlet dioxygen. Therefore, it could ultimately produce all ground-state products. The propagation channels are favored by higher temperatures, while lower temperatures favor the ISC-mediated production of ^1H_2CO, CH_3OH, and $^3O_2$. A fairly good qualitative agreement with the experimental T-dependence of the relevant branching ratio was then found. From the tetroxide over again (Scheme 3, right), dissociation of a single external O–O bond leads to $CH_3O^\bullet$ and $CH_3O_3^\bullet$, or possibly to a $^1(CH_3O^\bullet \cdots CH_3O_3^\bullet)$ complex, but further transformations along this line were not found to be competitive. We also looked for a concerted process leading from the tetroxide to the products, but a fully concerted (synchronous or asynchronous) "Russell TS", apt to connect it with formaldehyde, methanol, and dioxygen could not be found (center of Scheme 3 and Scheme 4).

Recently, the study of the evolution of aromatics under oxidation conditions has been further extended to polycyclic aromatic hydrocarbons (PAHs). These compounds, and their functionalized derivatives (PACs) are of great interest, mainly because many of them are of concern as regards human health, since they are mutagenic or carcinogenic compounds. For this reason, among various functionalizations, nitration is of particular interest. PAHs and PACs share with carbonaceous particulate the origin (combustion) and the structural nature. Their similarity explains why PACs are commonly found associated with soot. This interaction is of special concern, since ultrafine soot particles carrying adsorbed PACs can penetrate deeply into our respiratory system.

Consequently, we have been carrying out (recently and still at present) some theoretical studies along the following interrelated directions, aiming to:

(a) Model a soot platelet and its interactions with simple molecules of atmospheric interest.
(b) Investigate the mechanism by which PAHs and soot react with ozone.
(c) Investigate the nature of the oxidized soot surface.
(d) Describe the mechanistic details of nitration for some simple aromatics (benzene, naphthalene, pyrene, etc.)

(a) To begin with, graphite, and particularly defective graphite, was chosen to model a graphenic portion of a soot platelet. Quantum mechanical calculations were carried out first on molecular PAH-type systems, and then extended to a periodic representation of one graphite layer [34]. The features of the interaction of H, HO, NO, NO_2, and NO_3 with these model systems were then examined, with the purpose of defining a suitable representation of the atmospheric or combustion gas–solid interactions by which functionalization reactions can take place. The genuine solid-state effect, that in principle can be treated only with periodic models, regards only the π system of electrons, while the more interesting interactions with small reactive molecules regard σ orbitals, both at the edge of a graphene layer and at carbon vacancies (holes) within the sheet. The interaction with σ orbitals are more localized, and can be described well with molecular models of sufficient dimension, as those chosen, made up of 24 and 42 carbon atoms. The more interesting interactions with small reactive molecules regard the edge of the graphene sheet and the in-plane carbon vacancies. While these

interactions can be well described by sufficiently extended molecular models, periodic models are necessary to describe accurately the equilibrium geometries, because they introduce the necessary geometric constraints, while the molecular models allow a larger geometrical freedom. This preliminary study allowed us to show that the most interesting possible interaction of a graphenic model with the small molecules, present in tropospheric chemistry or combustion processes, are based on the ability of a graphene sheet to easily accommodate unpaired electrons in σ or π orbitals.

(b) Then, we extended the study by investigating in great detail the ozonization mechanism for PAHs and soot platelets. [35] This particular aspect was again studied by quantum mechanical calculations carried out on molecular and periodic systems. Both simulations of the oxidation processes of these substrates involve only exposed internal positions, i.e. they explicitly exclude the carbon atoms located along the perimeter of the platelet (which will be the object of a forthcoming study). The electrophilic attack by ozone is carried out in two ways. A concerted addition leads to a primary ozonide (PO), whilst a non-concerted attack produces a trioxyl diradical (TD, in which one of the two unpaired electrons is π-delocalized). Though some different possible pathways and intermediates were considered, only PO and TD were found as energy minima. Easy loss of (i) $^1O_2$, or (ii) $^3O_2$ from either intermediate, with spin conservation, would yield stable (i) singlet or (ii) triplet π-delocalized species which carry an epoxide group (EPO). In both cases, upon exoergic dioxygen loss, an overall energy barrier is overcome, estimated, for the more favorable case, 22, 21, and 14 kcal mol^{-1} high, for the three molecular models of increasing size. Thus, the process becomes easier upon extension of the unsaturated system. The TD pathway is probably preferred, though, in reality, the intervention of the diradical as a real intermediate is questionable, due to its easy re-dissociation. Rather, we can imagine that a "diradicaloid zone" of the energy hypersurface is probed by the reacting system. If the spin multiplicity is conserved, either a $^1\Delta_g$ oxygen molecule moves off the singlet functionalized substrate, or, as an alternative, ground-state dioxygen and a π-triplet epoxide might form. An intersystem crossing (ISC), taking place in the trioxyl diradical zone, can be invoked [36] to allow the even easier loss of a ground-state oxygen molecule with formation of a ground-state epoxide in a more exoergic and less demanding step. This is suggested by the fact that the triplet and singlet states of this intermediate have very similar energies, geometries, and vibrational frequencies. We propose that soot ozonization can take place by such a process, with ultimate functionalization of the graphenic platelets by epoxide groups. If the rate of formation for EPO is defined as $\nu_{EPO} = \nu_{TCD} + \nu_{PO}$, a steady-state treatment of the R–TD–EPO versus the R–PO–EPO pathways gives an estimate for the ν_{TCD}/ν_{PO} ratio of 10^{10}–10^{13}. It is then concluded that ozonization of internal positions has to pass through that region of the energy hypersurface where the system has diradical character. If an atmospheric process is considered, the barriers for the first attack appear to be too high to allow the ozonization of internal positions in a significant way, at least for the smallest PAHs and soot platelets. On the other hand, in an experiment employing large ozone concentrations, as that carried out by Schurath and coworkers [37], we can surmise that it can take place, but border ozonization (whose study is under way) should precede the massive ozonization of the internal positions.

(c) Here we will give a brief account of some work just concluded [38] on the features of the oxidized soot surface. We have made reference to a series of temperature-programmed desorption (TPD) experiments, and carried out a theoretical study of the desorption mechanisms involving oxygenated functionalities by using some PAC models. Substituents on PACs of increasing size (up to 46 carbon atoms in the parent PAH) are chosen to reproduce the local features of an oxidized graphenic soot platelet. Initially, the study is carried out on monomolecular fragmentation processes producing HO, CO, or CO_2, in some ketones, one aldehyde, some carboxylic acids, lactones, and anhydrides, one peroxyacid, one hydroperoxide, one secondary alcohol, and one phenol. Then, a bimolecular process is considered for one of the carboxylic acids. Finally, cooperative effect that can take place by involving two vicinal carboxylic groups (from anhydride hydrolysis) are investigated in other bifunctional models. The comparison between the computed fragmentation (desorption) barrier heights for the hypothesized mechanisms, and the temperature at which a maximum occurs in experimental TPD spectra (for HO, CO, or CO_2 desorption) offers a suggestion for the assignment of these maxima to specific functional groups.

(d) We have also undertaken a theoretical mechanistic study on the gas-phase nitration of aromatics,

beginning with the simplest cases: benzene (B) and naphthalene (N). Also this work is just concluded [39]. Nitration is considered to occur under tropospheric or combustion conditions. We are presently extending the investigation to anthracene, pyrene, acenaphtylene, cyclopenta[*cd*] pyrene, and phenantrene, with the main scope of assessing the effects of temperature. In principle, functionalization can either occur by direct nitration (NO_2 or N_2O_5 attack) or be initiated by more reactive species, as the nitrate and hydroxyl radicals. The attack of the NO_2 radical on B and N, followed by abstraction of the H geminal to the nitro group (most likely accomplished by $^3O_2$) can yield the final nitro-derivatives. However, the first step (NO_2 attack) involves significant free energy barriers. N_2O_5 proves to be an even worse nitrating agent. These results rule out direct nitration at room temperature. NO_3 can open an alternative pathway, through the formation of the π-delocalized nitroxycyclohexadienyl radicals. Similarly, and even more easily, HO can form the hydroxycyclohexadienyl radicals. A subsequent NO_2 attack on these intermediates can produce several regio- and diastereomers of the nitroxy-nitro or hydroxy-nitro closed-shell derivatives. If the two substituents are 1,2-*trans*, either a HNO_3 or H_2O concerted elimination can produce the final nitro-derivatives. HNO_3 elimination results feasible, while, by contrast, H_2O elimination presents a high barrier. If a combustion situation is hypothesized, the direct nitration pathway is put on a slightly better ground, yet it remains a very minor channel, at least for the nitration of the simplest aromatics, B and N.

The oxygen molecule in its first degenerate state ($^1\Delta_g$)O_2, $^1O_2$ for short, already encountered in the disproportionation step of the self-reaction of alkyl peroxyl radicals, is an ubiquitous reactive species in oxidation reactions [40]. It exhibits a diverse reactivity with organic unsaturated molecules (very different from that of the ground state, $^3O_2$), giving particularly the $[\pi 2 + \pi 2]$ and $[\pi 4 + \pi 2]$ cycloadditions. Moreover, wherever an allylic hydrogen is available, an additional reaction channel is available, the *ene* reaction, which produces a hydroperoxide. These different reactions can compete, but one usually dominates in particular circumstances. Given its synthetic interest, singlet dioxygen is produced on purpose and rather easily, frequently exploiting photosensitizers.

Its intervention has been also invoked in some photooxidation reactions involving PAHs as benzo[a]anthracene, benzo[a]pyrene (BaP), or cyclopenta[cd]pyrene. These are reactions of environmental interest because photodegradation is one major pathway for four- to six-ring PAHs in ambient aerosol [41]. Here, to illustrate the connection between atmospheric oxidations and the chemistry of singlet oxygen, we will only mention the mechanism suggested by Kahn and coworkers [42], later on confirmed by the experiments of Eisenberg and coworkers [43], for the so-called autooxidation of BaP (Scheme 5).

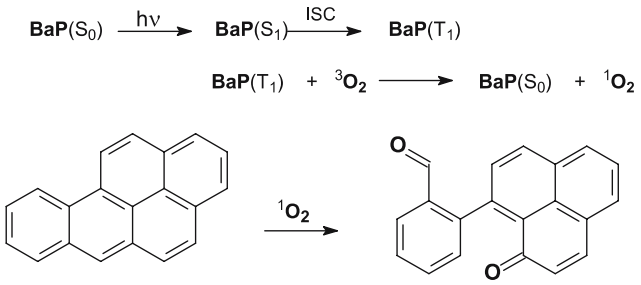

Scheme 5

The reactions of $^1O_2$ with organic unsaturated molecules are related by the possibility of sharing a common open-chain diradical/zwitterionic or cyclic perepoxide (also called peroxirane) intermediate. The reaction pathways are sketched in Scheme 6. For the *ene* reaction, both two-step and concerted mechanisms have been proposed in the past.

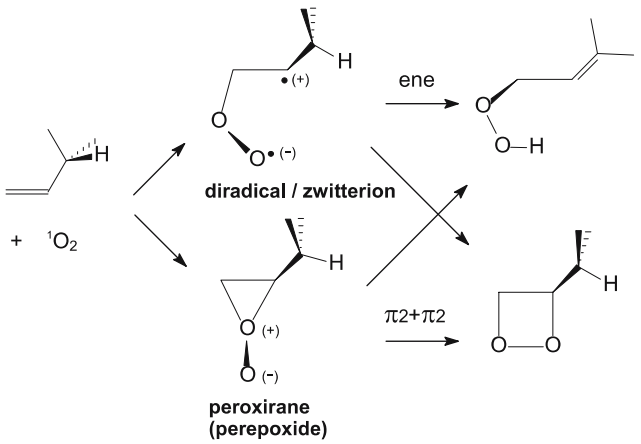

Scheme 6

The main purpose of the first study on the singlet oxygen reactions with alkenes [44] (which had been preceded in less recent times by an initial study of the simple singlet oxygen + ethene reaction) [45] is to assess the relative importance of diradical or peroxirane intermediates in the cycloaddition that lead to dioxetanes. The relevant pathways were explored for ethene, methyl

vinyl ether, and *s-trans* butadiene by multi-configurational methods (CAS-MCSCF optimizations followed by multi-reference perturbative CAS-PT2 energy calculations) and by DFT(B3LYP) optimizations. The two theoretical approaches produced similar results. Although the set of CH_2=CHX substrates considered in that study was limited to the three cases X=H, OCH_3, and CH=CH_2, the same qualitative description of the $[\pi 2 + \pi 2]$ reaction mechanism was obtained in all cases: methoxy or vinyl substitution does not affect qualitatively the reaction features found for the unsubstituted system. The main result is that peroxirane comes out to be attainable only by passing through the diradical, due to the nature of the critical points involved. The energy barriers for the transformation of the diradical to peroxirane ($\Delta E^{\ddagger} = 12$–15 kcal mol^{-1}) are higher than those for the diradical closure to dioxetane ($\Delta E^{\ddagger} = 8$–9 kcal mol^{-1}). In all three systems, the peroxirane pathway to dioxetane is prevented by the high energy barrier for the second step, leading from peroxirane to dioxetane ($\Delta E^{\ddagger} = 22$–31 kcal mol^{-1}). By contrast, peroxirane can very easily back-transform to the diradical (with a $\Delta E^{\ddagger}$ estimate of 3 kcal mol^{-1}, for ethene and methyl vinyl ether, and close to zero for butadiene). These results indicated that, although a peroxirane intermediate might form in some cases, it corresponds to a dead-end pathway which cannot lead to dioxetane.

The research was then extended by taking into account the pathway leading to a hydroperoxide (ene reaction) in the simple propene model, at the CAS(12,12)-PT2//CAS(10,8)-MCSCF or CAS(12,12)-PT2//CAS(12,10)-MCSCF theory levels [46]. This approach was flanked by a series of DFT calculations employing two different functionals: B3LYP and MPW1K. This second study aimed to determine if a balance between concerted and non-concerted pathways exists, and in particular to ascertain again the possible role of diradical/zwitterion or peroxirane intermediates. Three non-concerted pathways, via (1) diradical or (2) peroxirane intermediates, and (3) via H-abstraction/radical recoupling, plus one concerted pathway (4), are explored. (1) The polar diradical forms from the separate reactants by getting through a barrier ($\Delta E^{\ddagger}_{MPW1K} = 12$, $\Delta E^{\ddagger}_{B3LYP} = 14$, and $\Delta E^{\ddagger}_{CASPT2} = 16$ kcal mol^{-1}) and can back-dissociate through the same TS, with barriers of 11 (MPW1K) and 8 kcal mol^{-1} (B3LYP and CASPT2). The diradical can easily transform into the hydroperoxide at all levels ($\Delta E^{\ddagger}_{MPW1K} < 4$, $\Delta E^{\ddagger}_{B3LYP} = 1$ and $\Delta E^{\ddagger}_{CASPT2} = 1$ kcal mol^{-1}). Diradical formation is described as not reversible, and the relevant pathway comes out to be sharply favored. (2) Peroxirane is found again to be attainable only by passing through the diradical intermediate, and not directly, due to the nature of the critical points involved. It is located higher in energy than the diradical by 12 kcal mol^{-1}, at all theory levels. The energy barrier for the diradical to *cis*-peroxirane transformation is much higher than that for the diradical transformation to the hydroperoxide. Moreover, peroxirane is inclined to very easily back-transform to the diradical ($\Delta E^{\ddagger} < 3$ kcal mol^{-1}). Both the energetics and the qualitative characteristics of the energy hypersurface preclude at all levels the existence of a peroxirane-to-hydroperoxide channel. Of course, further investigation on more complex systems is advisable before taking this result for general. (3) An alternative two-step pathway (H-abstraction by $^1O_2$, followed by HOO-allyl radical coupling) is not competitive with the diradical mechanism. (4) A concerted pathway, flanking the non-concerted diradical pathway, and connecting directly the reagents to the hydroperoxide, was suggested by a restricted DFT calculation. It was carefully investigated, and discarded as an artifact of the restricted scheme. Finally, the ene/$[\pi 2 + \pi 2]$ possible competition was considered. The cycloaddition pathway stems from the same diradical intermediate, but cannot compete in this system with the very easy *ene* step, which is preferred by a factor of ca. 10^3. Given that the cycloaddition TS is slightly more polar than the ene, we attempted to simulate the effect of a polar solvent (CH_3CN) by two methods, to asses its effectiveness in tuning the competition more in favor of the cycloaddition. One simulation gave a very small effect in that sense, while the other was basically ineffective.

Since cyclic peroxiranes are often postulated as common polar intermediates in the reactions of $^1O_2$ with alkenes, we addressed in particular the significance of trapping experiments, which had been used as a basis to maintain the intermediacy of perepoxides [47]. These experiments exploit the capability of reducing agents to extract an oxygen atom from the putative perepoxide, to generate an epoxide. This theoretical study (in which trimethyl phosphite has been chosen as a representative electrophilic reducing agent) showed that trapping experiments cannot distinguish between a peroxirane and an open-chain intermediate pathway, because an epoxide is the shared outcome of any attack by the reducing molecule. In conclusion such an experiment cannot demonstrate in a compelling way the intervention of peroxirane.

Finally, we have studied some interesting features of the *ene* reaction of singlet oxygen with $\alpha,\beta-$unsaturated carbonyl compounds [48]. The *s-cis* and *s-trans* reactants show different reactivities in producing unsaturated hydroperoxides. Moreover, a marked regioselectivity is

observed, which is influenced to some extent by solvent polarity. These characteristics are nicely accounted for by a polar diradical mechanism. This mechanism seems apt to interpret correctly both the observed regiochemistry and the relative reactivity of the *s-cis* and *s-trans* conformers of the reactant (E)-2-methylbut-2-enal. On one hand, the regioselectivity originates from the different stabilities of the two diradical intermediates obtained by O_2 addition. The higher reactivity of *s-cis* species with respect to the *s-trans* is due to the greater stability of the *s-trans* conformation, while the rate-determining step corresponds to transition structures of similar stability. The computed kinetic isotope effect ($k_H/k_D = 1.2$) is in fairly good agreement with the value measured for a similar substrate ($k_H/k_D = 1.30$ for methyl (E)-2-methylbut-2-enoate in benzene). The solvent effect on the energy barriers is small, and favors the addition on the β carbon. A perepoxide intermediate is not a critical point on this reaction's potential energy hypersurface. Furthermore, a trioxene intermediate is located too high in energy to be significantly populated. An alternative pathway leading to dioxetane (the $[\pi 2 + \pi 2]$ cycloaddition reaction) is not as effective as the ene pathway giving the hydroperoxide.

References

1. Roos BO, Taylor PR, Siegbahn PEM (1980) Chem Phys 48:157–173
2. Roos BO (1987) The complete active space self-consistent field method and its applications in electronic structure calculations. In: Lawley KP (ed) Ab initio methods in quantum chemistry-II. Wiley (The implementation of this kind of approach in the Gaussian program system is documented in Hegarty D, Robb MA (1979) Mol Phys 38:1795–1812)
3. Eade RHA, Robb MA (1981) Chem Phys Lett 83:362–368
4. Andersson K, Malmqvist P-Å, Roos BO, Sadlej AJ, Wolinski K (1990) J Phys Chem 94:5483–5488
5. Andersson K, Malmqvist P-Å, Roos BO (1992) J Chem Phys 96:1218–1226
6. Roos BO, Andersson K, Fülscher MP, Malmqvist P-Å, Serrano-Andres L, Pierloot K, Merchán M (1996) Adv Chem Phys 93:219–331
7. Nakano H (1993) Chem Phys Lett 207:372–378
8. Nakano H (1993) J Chem Phys 99:7983–7992
9. Parr RG, Yang W (1989) Density functional theory of atoms and molecules. Oxford University Press, New York, chap 3
10. Becke AD (1988) Phys Rev A 38:3098–3100
11. Becke AD (1989) ACS Symp Ser 394:165–173
12. Pople JA, Gill PMW, Johnson BG (1992) Chem Phys Lett 199:557–560
13. Becke AD (1993) J Chem Phys 98:5648–5652
14. Lee C, Yang W, Parr RG (1988) Phys Rev B 37:785–789
15. Basch H, Hoz S (1997) J Phys Chem A 101:4416–4431
16. Baker J, Muir M, Andzelm J (1995) J Chem Phys 102: 2063–2079
17. Handy NC, Knowles PJ, Somasundram K (1985) Theor Chim Acta 68:87–100
18. Baker J, Scheiner A, Andzelm J (1993) Chem Phys Lett 216:380–388
19. Baker J, Andzelm J, Muir M, Taylor PR (1995) Chem Phys Lett 237:53–60
20. Jursic B (1996) Chem Phys Lett 256:603–608
21. Ghigo G, Tonachini G (1999) J Chem Phys 110:7298–7304
22. Seeger R, Pople JA (1977) J Chem Phys 66:3045–3050
23. Bauernschmitt R, Ahlrichs R (1996) J Chem Phys 104:9047–9052
24. Schlegel HB, McDouall JJ (1991) In: Ogretir C, Csizmadia IG (eds) Computational advances in organic chemistry. Kluwer Academic, Dordrecht, p 167
25. Jungkamp TPW, Seinfeld JH (1996) Chem Phys Lett 257:15–22
26. Jungkamp TPW, Seinfeld JH (1996) Chem Phys Lett 259:683 (erratum)
27. Jungkamp TPW, Seinfeld JH (1996) Chem Phys Lett 263:371–378
28. Ghigo G, Tonachini G (1998) J Am Chem Soc 120:6753–6757
29. Ghigo G, Tonachini G (1999) J Am Chem Soc 121:8366–8372
30. Motta F, Tonachini G (2001) in Atmospheric diagnostics in urban regions. Series: Initiativen zum Umweltschutz—Initiatives for environmental protection, vol 33. Erich Schmidt, Berlin, pp 120–128
31. Motta F, Ghigo G, Tonachini G (2002) J Phys Chem A 106:4411–4422
32. Ghigo G, Motta F, Tonachini G (2002) Recent research developments in organic chemistry. Transworld Research Network, Trivandrum, pp 129–145
33. Ghigo G, Maranzana A, Tonachini G (2003) J Chem Phys 119:10575–10583
34. Ghigo G, Maranzana A, Tonachini G, Zicovich-Wilson CM, Causà M (2004) J Phys Chem B 108:3215–3223
35. Maranzana A, Serra G, Giordana A, Tonachini G, Barco G, Causà M (2005) J Phys Chem A 109:10929–10939
36. Borrelli R, Peluso A, Maranzana A, Causà M, Tonachini G (in preparation)
37. Kamm S, Mohler O, Naumann K-H, Saathoff H, Schurath U (1999) Atmos Environ 33:4651–4661
38. Barco G, Maranzana A, Ghigo G, Causà M, Tonachini G (2006) J Chem Phys 125:194706
39. Ghigo G, Causà M, Maranzana A, Tonachini G (2006) J Phys Chem A (in press)
40. Foote CS, Clennan EL (1995) Properties and reactions of singlet dioxygen. In: Foote CS, Valentine JS, Greenberg A, Liebman JF (eds) Active oxygen in chemistry. Blackie Academic and Professional (Chapmann & Hall), chap 4, pp 105–140
41. Finlayson-Pitts BJ, Pitts JN Jr (2000) Chemistry of the upper and lower atmosphere. Academic, New York, chap 10, Sect E.4
42. Pitts JN Jr, Khan A, Smith EB, Wayne RP (1969) Environ Sci Technol 3:241–247
43. Eisenberg WC, Taylor K, Murray RW (1984) Carcinogenesis 5:1095–1096
44. Maranzana A, Ghigo G, Tonachini G (2000) J Am Chem Soc 122:1414–1423
45. Tonachini G, Schlegel HB, Bernardi F, Robb MA (1990) J Am Chem Soc 112:483–491
46. Maranzana A, Ghigo G, Tonachini G (2003) Chem Eur J 9:2616–2626
47. Maranzana A, Ghigo G, Tonachini G (2003) J Org Chem 68:3125–3129
48. Maranzana A, Ghigo G, Canepa C, Tonachini G (2005) Eur J Org Chem 17:3643–3649